Supporting information

Nacre-Inspired Strong and Multifunctional Soy Protein-Based Nanocomposite Materials for Easy Heat-Dissipative Mobile Phone Shell

Shuaicheng Jiang,[†,‡] Yanqiang Wei,[†,‡] Sheldon Q. Shi,[§] Youming Dong,[†,‡] Changlei Xia,[†,‡] Dan Tian,[†,‡] Jing Luo,[†,‡] Jianzhang Li[,‡,⊥] and Zhen Fang*[,¶,#]*

[†]Jiangsu Key Open Laboratory of Wood Processing and Wood-based Panel Technology, Nanjing Forestry University, Nanjing, Jiangsu 210037, China

[‡]College of Materials Science and Engineering, Nanjing Forestry University, Nanjing, Jiangsu 210037, China

[§]Department of Mechanical Engineering, University of North Texas, Denton, TX 76203, United States

[⊥]MOE Key Laboratory of Wooden Material Science and Application, Beijing Forestry University, Beijing 100083, China

[¶]Department of Biochemistry & Molecular Biology, Michigan State University, 603 Wilson Road, East Lansing, Michigan, 48824, United States

[#]Great Lakes Bioenergy Research Center- Michigan State University, 1129 Farm Lane, East Lansing, Michigan, 48824, United States

*Correspondence to: lijzh@bjfu.edu.cn (J. Li)

fangzhe8@msu.edu (Z. Fang)

Table of Contents

Experimental.....S3

Characterization of the SPI-BN and SPI-GL.....S5

Comparison of the SPI-BN with different materials in other studies.....S9

References S14

Experimental

Materials. SPI (95% protein) was obtained from Yuwang Ecological Food Industry Co., Ltd. (Shandong, China). Hydrogen peroxide (30 wt%), glycerol (AR) and sodium hydroxide (NaOH, AR) were supplied by Nanjing Chemical Reagents Co., Ltd. (Nanjing, China). Trimethylolpropane triglycidyl ether (TTE, Epoxy value/100 g : 0.70), boron nitride (99.9% metals basis, 1-2 μm), and other chemicals were supplied by Aladdin Biochem Co., Ltd. (Shanghai, China). All chemicals were used without further purification. Deionized water was used for all experiments.

Preparation of BN-OH nanosheets. BN-OH nanosheets were prepared using a previously reported method.[1] The BN nanosheets were dispersed in deionized water (0.5 wt%) and stirred thoroughly for 24 h, followed by an ultrasonic treatment for 0.5 h. Finally, the suspension was filtered to remove the unabsorbed BN.

Preparation of SPI-based nanocomposite films. a) Preparation of SPI-GL. A mixture of SPI (5 g) and glycerol (GL, 2.5 g) was added to 95 mL of distilled water, and the resulting solution was stirred vigorously for 10 min at room temperature. The pH was then

adjusted to 10 with a NaOH solution (10% (w/w)) and the mixture was heated at 85 °C for 30 min (with magnetic stirring). After 30 min of sonification and degassing, the resulting solution was poured into Teflon-coated plates and dried in a vacuum oven at 45 ℃ for 48 h; b) Preparation of SPI-BN. SPI (5 g) was added to the above BN-OH solution (100 g) under vigorous mechanical stirring for 1 h. Subsequently, trimethylolpropane triglycidyl ether (TTE, 1 g) were added into the system (pH 9.0; water bath at 85 ℃) for 30 min until a homogeneous mixture solution was attained. After 30 min of sonification and degassing, the resulting solution was poured into Teflon-coated plates and dried in a vacuum oven at 45 ℃ for 48 h.

The formulated SPI-GL and SPI-BN above were peeled off and stored in a desiccator (25 ℃ and 50% relative humidity) for subsequent testing. The synthesis process and enhancement mechanism for the SPI-BN is shown in Figure 1.

Characterization of SPI-BN and SPI-GL. The bonding characteristics in SPI, BN, and SPI-BN were examined using Fourier transform infrared spectroscopy (FTIR, Nicolet iS50 Thermo Fisher Scientific Co., Ltd, USA). FTIR spectra were recorded from 500 to 4000

cm^{-1} with a resolution of 4 cm^{-1} at ambient temperature for 32 scans. Rheological test was carried out on an RST-CPS rheometer using a 50 mm parallel-plate at room temperature. The elemental compositions and chemical structures of SPI-BN nanocomposite film were examined by X-ray photoelectron spectroscopy (XPS, AXIS UltraDLD, Britain) and X-ray diffraction patterns (XRD, Ultima IV analyzer, Rigaku, Japan). Thermogravimetric analysis (TGA) of the SPI-based nanocomposite film (around 5 mg) were performed on a TGA55 instrument (Waters, USA) in the temperature range of 25-800 °C at a heating rate of 10 °C min^{-1} under N_2 with a flow rate of 100 mL min^{-1}. The UV-vis absorption spectra were obtained for the 200-800 nm range using a UV lamp (PE Lambda950). The samples were cut into rectangles (5 cm × 2 cm). Morphology and structure of films were observed with scanning electron microscope (SEM, Quanta 200, USA). The thermal conductivity (K) was calculated by $K=\alpha \cdot \rho \cdot C_p$, where α, ρ, and C_p were the thermal diffusivity, measured density and specific heat capacity of the sample, respectively, which could be measured by laser flash technique (LFA 467, Netzsch). The electromagnetic interference shielding property of the SPI-BN nanocomposite film in the frequency range

of 8.2-12.4 GHz (X band) was investigated by a vector network analyzer (E5071C) using a waveguide method. The SE was calculated by the following equations.

$SE_T = SE_R + SE_A + SE_M$

$SE_R = -10\lg(1-R) = -10\lg(1-(S_{11})^2)$

$SE_A = -10\lg(T/1-R) = -10\lg((S_{21})^2/1-(S_{11})^2)$

The SE_T is the sum of reflection (SE_R), absorption (SE_A), and multiple reflections (SE_M).

Mechanical testing of SPI-BN and SPI-GL. The mechanical performance of the composites was evaluated using an electron universal testing machine (AGS-X, Japan). Film samples with dimensions of 10 × 80 mm (width × length) were tested at a tensile speed of 20 mm/min. All tests were conducted in quintuplicates. The dynamic mechanical behavior of the composites was analyzed on a dynamic thermomechanical analyzer (DMA, Q850, TA Instruments, USA) in tensile mode at a frequency of 1 Hz. The composites were tested from 20 to 180 °C at a heating rate of 5 °C min^{-1} under an air atmosphere.

Characterization of the SPI-BN and SPI-GL

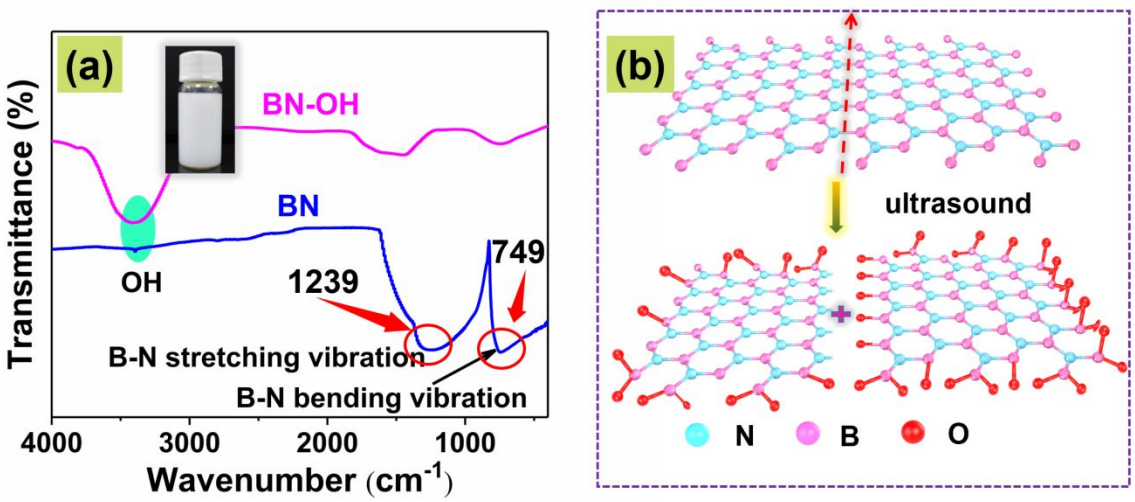

Figure S1. (a) FTIR spectra of BN and BN-OH. (b) Functionalization of BN to BN-OH.

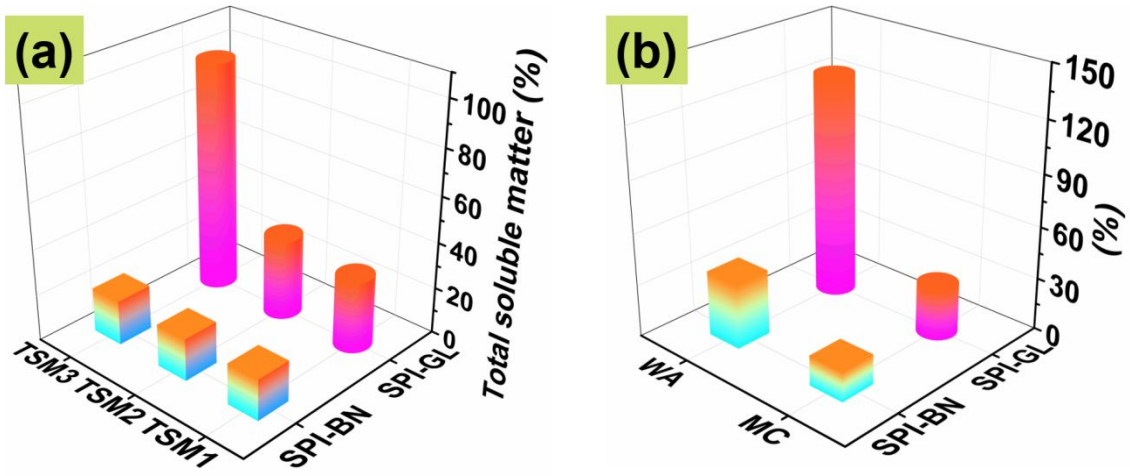

Figure S2. (a) Total soluble matter of SPI-GL and SPI-BN (TSM1: in water at 30 ℃ for 1 h; TSM2: in water at 63 ℃ for 3 h; TSM3: in water at 100 ℃ for 3 h). (b) Water

absorption (WA) at 95% relative humidity (30 ℃) and moisture content (MC) of SPI-GL and SPI-BN.

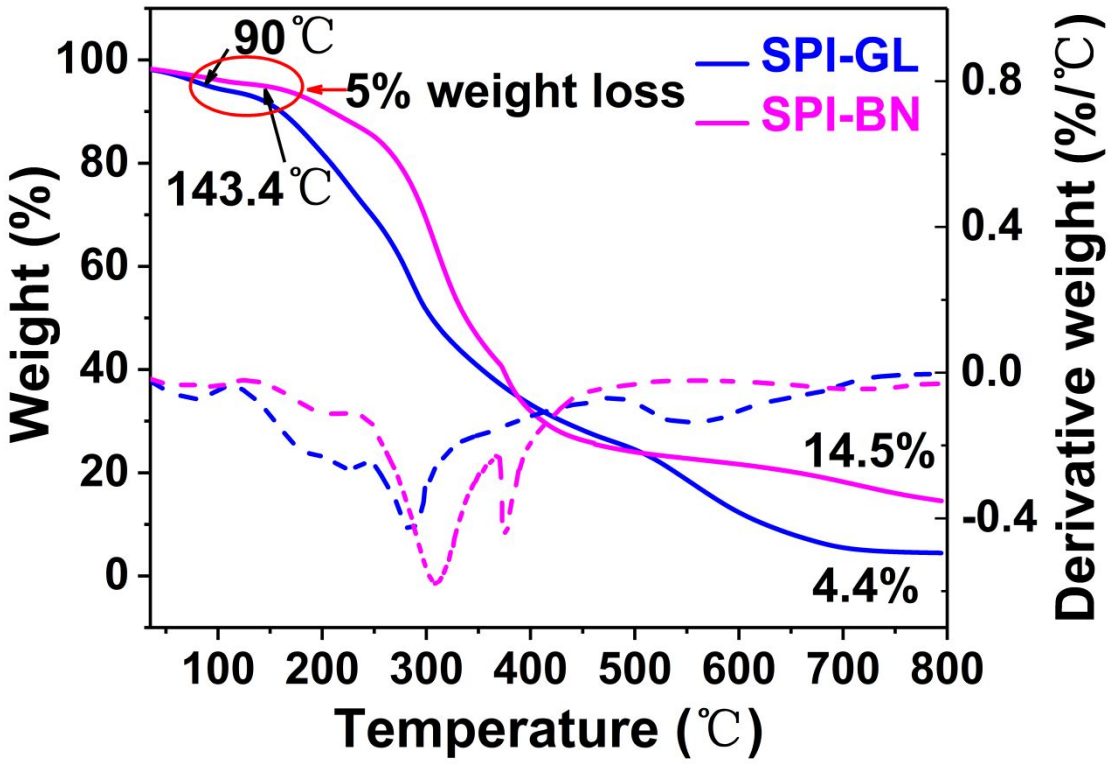

Figure S3. TG and DTG curves of SPI-GL and SPI-BN.

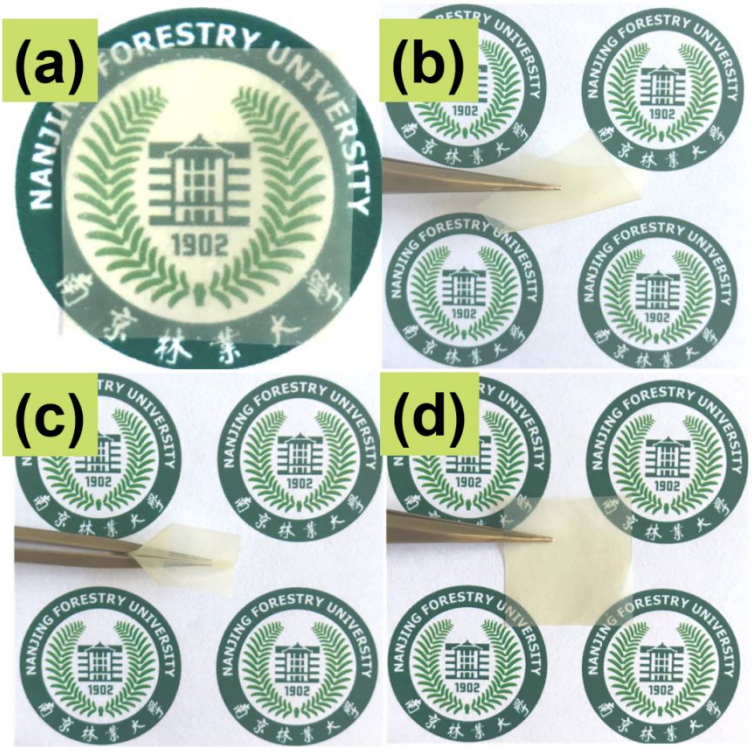

Figure S4. (a) Photo of a transparency SPI-BN. (b and c) Folded into a paper airplane shape.

(d) The folded film recovered to its original shape without observable damage. Permission to use the logo has been granted by college of Materials Science and Engineering, Nanjing Forestry University (Nanjing, Jiangsu, China).

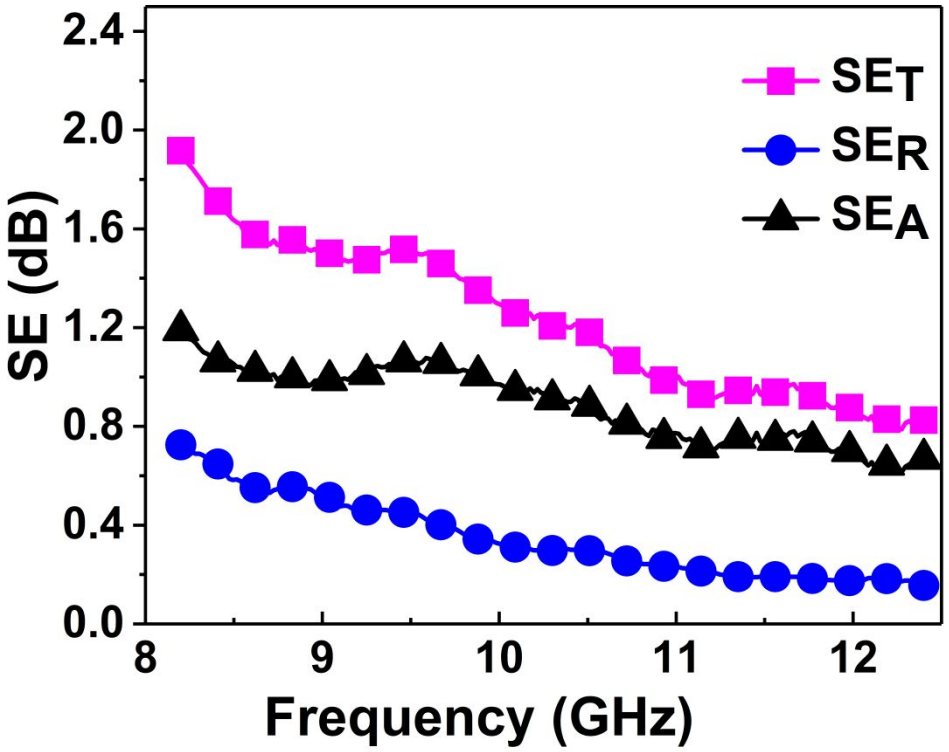

Figure S5. Comparison of SE_T, SE_R, and SE_A of the SPI-BN in the transverse direction in the X band.

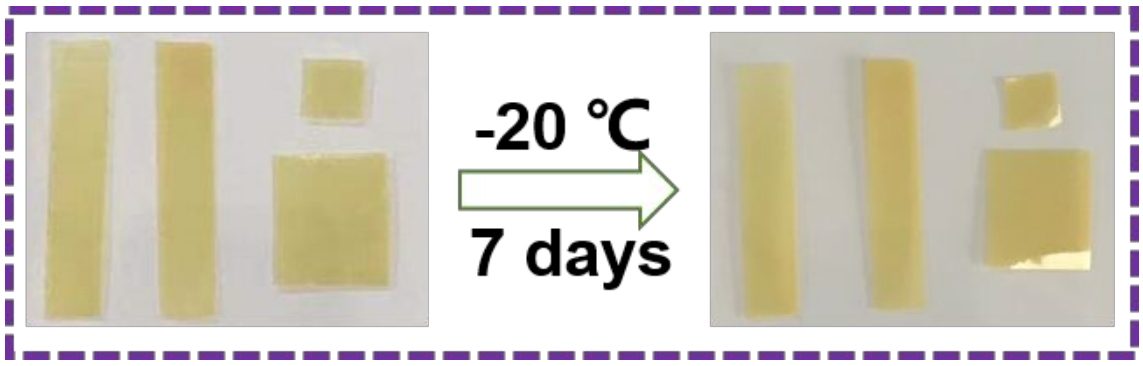

Figure S6. Appearance of SPI-BN under low temperature (-20 °C) for 7 days.

Comparison of the SPI-BN with different materials in other studies

Table S1. Mechanical properties of SPI-GL and SPI-BN

Samples	strain at break (%)	tensile strength (MPa)	Young's modulus (MPa)	tensile toughness (MJ/m^3)	impact strength (KJ/m^2)
SPI-GL	100.5	2.64	82.1	2.42	-
SPI-BN	13.3	36.4	529.2	2.58	5

Table S2. Tensile strength of SPI-GL, SPI-BN and other nanocomposite materials.

Composites	strain at break (%)	tensile strength (MPa)	Refs
TA@CNF	11.6	16	2
Rapeseed oil	4.2	1.9	3
Agar	38.89	13.62	4
Chitosan	30.8	5.0	5
GO/HPPy	85.6	12.3	6
HPPy@CNF	127.6	13.4	7
ZnO nanorod	12.64	14.74	8
SPI/MMT	5	8.5	9
SPI-CNPC	61.89	13.19	10
FBN	3.1	7	11
FBN/PVA	0.8	21.2	11
ASP/CMC	20	5.97	12
SPI-GL	100.5	2.64	This work
SPI-BN	13.3	36.4	This work

Table S3. Comparison of the in-plane thermal conductivity (TC) of SPI-BN with different composites materials.

Filler	Matrix	Filler loading (wt %)	TC ($W \cdot m^{-1} \cdot K^{-1}$)	Refs
BN/Diamond	Polyimide	40	0.98	13
BN/Al_2O_3	Epoxy	50	0.808	14
BN	Polyimide	30	1.2	15
BNNS	PI	5.1	1.47	16
RGO/BNNS	PI	1	1.54	16
MBN	PCL	5	0.55	17
3D graphene	Polyimide	0.35	1.7	18
3D graphene	PDMS	0.7	0.56	19
3D graphene	PMMA	2.5	0.7	20
3D graphene	Epoxy	0.92	2.13	21
BN	SPI	0.5	2.40	This work

Table S4. The specific thermal conductivity (STC, = TC/Filler loading (%)) of SPI-BN with different composites material.

Filler	Matrix	Filler loading (wt %)	STC ($W \cdot m^{-1} \cdot K^{-1}$)	Refs
BN/Diamond	Polyimide	40	2.5	13
BN	Polyimide	60	11.7	22
BN/Al_2O_3	Epoxy	50	1.6	14
BN	Polyimide	30	4.0	15
BN	PVA	30	14.7	23
BN	PMMA	24	13.2	24
BN	Epoxy	40	14.7	25
Graphene/BN	Epoxy	44	25.0	26
3D BN	Epoxy	24.4	21.3	27
BNNS	PI	5.1	28.8	16
RGO/BNNS	PI	1	154.0	16
MBN	PCL	5	11.0	17
BN	PDMS	16	69.1	28
ANF/BNNS	ANF	30	155.7	29
3D graphene	PDMS	0.7	80.0	19
3D graphene	PMMA	2.5	28.0	20
3D graphene	Epoxy	0.92	231.5	21
SiC/graphene	Polyimide	11	23.9	13
BN	SPI	0.5	480.0	This work

Table S5. Comparison of thermal conductivity (TC) of SPI-BN with typical polymers from previous studies.[30-34]

Typical polymers	TC ($W \cdot m^{-1} \cdot K^{-1}$)
Polystyrene (PS)	0.12 ± 0.005
Polypropylene (PP)	0.13 ± 0.03
Polyester	0.135 ± 0.005
Polyethylene terephthalate (PET)	0.14 ± 0.005
Acrylic (PMMA)	0.16 ± 0.08
Polycarbonate (PC)	0.21 ± 0.015
Teflon (PTFE)	0.21 ± 0.07
Polyvinyl Chloride (PVC)	0.22 ± 0.005
Nylons (PA)	0.23 ± 0.01
Polyetherether ketone (PEEK)	0.25 ± 0.01
Epoxies	0.25 ± 0.01
Acrylonitrile butadiene styrene (ABS)	0.26 ± 0.08
Acetal (POM)	0.28 ± 0.06
Polyurethane thermoplastics (TPU)	0.29 ± 0.01
Phenolics	0.32 ± 0.18
Polyethylene (PE)	0.42 ± 0.02
SPI-BN (This work)	2.4 ± 0.1

Table S6. Comparison of thermal conductivity (TC) of SPI-BN with different mobile phone shell materials.[32-34]

Materials	TC ($W \cdot m^{-1} \cdot K^{-1}$)
Flannelette	0.05 ± 0.01
Wood	0.12 ± 0.03
Polyurethane thermoplastics (TPU)	0.13 ± 0.01
Acrylic (PMMA)	0.18 ± 0.01
Leather	0.18 ± 0.015
Polycarbonate (PC)	0.2 ± 0.012
Polypropylene (PP)	0.23 ± 0.01
Silica gel	0.5 ± 0.008
Glass	1 ± 0.02
SPI-BN (This work)	2.4 ± 0.1

Table S7. Comparison of mechanical of SPI-BN with different mobile phone shell materials.[32-34]

Materials	Young's modulus (GPa)	tensile strength (MPa)
Leather	0.1-0.5	20-26
Wood, typical (transverse)	0.5-3	4-9
Cork	0.013-0.05	0.5-2.5
Acrylonitrile butadiene styrene (ABS)	1.1-2.9	27.6-55.2
Polyethylene (PE)	0.621-0.896	20.7-44.8
Polypropylene (PP)	0.896-1.55	27.6-41.4
Polystyrene (PS)	2.28-3.34	35.9-56.5
Polyurethane thermoplastics (TPU)	1.31-2.07	31-62
Teflon (PTFE)	0.4-0.552	20-30

Rigid polymer foam (HD)	0.2-0.48	1.2-12.4
Borosilicate glass	61-64	22-32
Soda-lime glass	68-72	31-35
SPI-BN (This work)	0.53	36.4

References

(1) Qi, X.; Yang, L.; Zhu, J.; Hou, Y.; Yang, M., Stiffer but More Healable Exponential Layered Assemblies with Boron Nitride Nanoplatelets. *ACS Nano* **2016**, *10*, 9434-9445.

(2) Wang, Z.; Wen, Y.; Zhao, S.; Zhang, W.; Ji, Y.; Zhang, S.; Li, J., Soy Protein as a Sustainable Surfactant to Functionalize Boron Nitride Nanosheets and Its Application for Preparing Thermally Conductive Biobased Composites. *Ind. Crop. Prod.* **2019**, *137*, 239-247.

(3) Li, K.; Jin, S.; Chen, H.; He, J.; Li, J., A High-Performance Soy Protein Isolate-Based Nanocomposite Film Modified with Microcrystalline Cellulose and Cu and Zn Nanoclusters. *Polymers. Basel.* **2017**, *9*, 167.

(4) Mohajer, S.; Rezaei, M.; Hosseini, S. F., Physico-Chemical and Microstructural Properties of Fish Gelatin/Agar Bio-Based Blend Films. *Carbohydr. Polym.* **2017**, *157*, 784-793.

(5) Li, K.; Jin, S.; Liu, X.; Chen, H.; He, J.; Li, J., Preparation and Characterization of Chitosan/Soy Protein Isolate Nanocomposite Film Reinforced by Cu Nanoclusters. *Polymers. Basel.* **2017**, *9*, 247.

(6) Jin, S.; Li, K.; Gao, Q.; Zhang, W.; Chen, H.; Shi, S. Q.; Li, J., Assembly of Graphene Oxide into the Hyperbranched Frameworks for the Fabrication of Flexible Protein-Based Films with Enhanced Conductivities. *Compos. Part. B-Eng.* **2020**, *196*, 108110.

(7) Marvizadeh, M. M.; Oladzadabbasabadi, N.; Mohammadi Nafchi, A.; Jokar, M., Preparation and Characterization of Bionanocomposite Film Based on Tapioca Starch/Bovine Gelatin/Nanorod Zinc Oxide. *Int. J. Biol. Macromol.* **2017**, *99*, 1-7.

(8) Li, K.; Jin, S.; Chen, H.; Li, J., Bioinspired Interface Engineering of Gelatin/Cellulose Nanofibrils Nanocomposites with High Mechanical Performance and Antibacterial Properties for Active Packaging. *Compos. Part. B-Eng.* **2019**, *171*, 222-234.

(9) Echeverria, I.; Eisenberg, P.; Mauri, A. N., Nanocomposites Films Based on Soy Proteins and Montmorillonite Processed by Casting. *J. Membrane. Sci.* **2014**, *449*, 15-26.

(10) Li, Y.; Chen, H.; Dong, Y.; Li, K.; Li, L.; Li, J., Carbon Nanoparticles/Soy Protein Isolate Bio-Films with Excellent Mechanical and Water Barrier Properties. *Ind. Crop. Prod.* **2016**, *82*, 133-140.

(11) Wang, J.; Wu, Y.; Xue, Y.; Liu, D.; Wang, X.; Hu, X.; Bando, Y.; Lei, W., Super-Compatible Functional Boron Nitride Nanosheets/Polymer Films with Excellent Mechanical Properties and Ultra-High Thermal Conductivity for Thermal Management. *J. Mater. Chem. C.* **2018**, *6*, 1363-1369.

(12) Choi, I.; Chang, Y.; Shin, S.-H.; Joo, E.; Song, H. J.; Eom, H.; Han, J., Development of Biopolymer Composite Films Using a Microfluidization Technique for Carboxymethylcellulose and Apple Skin Particles. *Int. J. Mol. Sci.* **2017**, *18*, 1278.

(13) Dai, W.; Yu, J.; Wang, Y.; Song, Y.; Alam, F. E.; Nishimura, K.; Lin, C.-T.; Jiang, N., Enhanced Thermal Conductivity for Polyimide Composites with a Three-Dimensional

Silicon Carbide Nanowire@Graphene Sheets Filler. *J. Mater. Chem. A.* **2015**, *3*, 4884-4891.

(14) Fang, L.; Wu, C.; Qian, R.; Xie, L.; Yang, K.; Jiang, P., Nano-Micro Structure of Functionalized Boron Nitride and Aluminum Oxide for Epoxy Composites with Enhanced Thermal Conductivity and Breakdown Strength. *Rsc. Adv.* **2014**, *4*, 21010-21017.

(15) Li, T.-L.; Hsu, S. L.-C., Enhanced Thermal Conductivity of Polyimide Films via a Hybrid of Micro- and Nano-Sized Boron Nitride. *J. Phys. Chem. B.* **2010**, *114*, 6825-6829.

(16) Guo, F.; Shen, X.; Zhou, J.; Liu, D.; Zheng, Q.; Yang, J.; Jia, B.; Lau, A. K. T.; Kim, J.-K., Highly Thermally Conductive Dielectric Nanocomposites with Synergistic Alignments of Graphene and Boron Nitride Nanosheets. *Adv. Funct. Mater.* **2020**, *30*, 1910826.

(17) Tian, H.; Wu, F.; Chen, P.; Peng, X.; Fang, H., Microwave-Assisted in Situ Polymerization of Polycaprolactone/Boron Nitride Composites with Enhanced Thermal Conductivity and Mechanical Properties. *Polym. Int.* **2020**, *69*, 635-643.

(18) Loeblein, M.; Bolker, A.; Tsang, S. H.; Atar, N.; Uzan-Saguy, C.; Verker, R.; Gouzman, I.; Grossman, E.; Teo, E. H. T., 3D Graphene-Infused Polyimide with Enhanced Electrothermal Performance for Long-Term Flexible Space Applications. *Small* **2015**, *11*, 6425-6434.

(19) Zhao, Y.-H.; Wu, Z.-K.; Bai, S.-L., Study on Thermal Properties of Graphene Foam/Graphene Sheets Filled Polymer Composites. *Compos. Part. A-Appl. S.* **2015**, *72*, 200-206.

(20) Fan, Z.; Gong, F.; Nguyen, S. T.; Duong, H. M., Advanced Multifunctional Graphene Aerogel - Poly (Methyl Methacrylate) Composites: Experiments and Modeling. *Carbon* **2015**, *81*, 396-404.

(21) Lian, G.; Tuan, C.-C.; Li, L.; Jiao, S.; Wang, Q.; Moon, K.-S.; Cui, D.; Wong, C.-P., Vertically Aligned and Interconnected Graphene Networks for High Thermal Conductivity of Epoxy Composites with Ultralow Loading. *Chem. Mater.* **2016**, *28*, 6096-6104.

(22) Sato, K.; Horibe, H.; Shirai, T.; Hotta, Y.; Nakano, H.; Nagai, H.; Mitsuishi, K.; Watari, K., Thermally Conductive Composite Films of Hexagonal Boron Nitride and Polyimide with Affinity-Enhanced Interfaces. *J. Mater. Chem.* **2010**, *20*, 2749-2752.

(23) Xie, B.-H.; Huang, X.; Zhang, G.-J., High Thermal Conductive Polyvinyl Alcohol Composites with Hexagonal Boron Nitride Microplatelets as Fillers. *Compos. Sci. Technol.* **2013**, *85*, 98-103.

(24) Zhi, C.; Bando, Y.; Terao, T.; Tang, C.; Kuwahara, H.; Golberg, D., Towards Thermoconductive, Electrically Insulating Polymeric Composites with Boron Nitride Nanotubes as Fillers. *Adv. Funct. Mater.* **2009**, *19*, 1857-1862.

(25) Liu, Z.; Li, J.; Liu, X., Novel Functionalized BN Nanosheets/Epoxy Composites with Advanced Thermal Conductivity and Mechanical Properties. *ACS Appl. Mater. Interfaces* **2020**, *12*, 6503-6515.

(26) An, F.; Li, X.; Min, P.; Li, H.; Dai, Z.; Yu, Z.-Z., Highly Anisotropic Graphene/Boron Nitride Hybrid Aerogels with Long-Range Ordered Architecture and Moderate Density for Highly Thermally Conductive Composites. *Carbon* **2018**, *126*, 119-127.

(27) Tian, Z.; Sun, J.; Wang, S.; Zeng, X.; Zhou, S.; Bai, S.; Zhao, N.; Wong, C.-P., A Thermal Interface Material Based on Foam-Templated Three-Dimensional Hierarchical Porous Boron Nitride. *J. Mater. Chem. A.* **2018**, *6*, 17540-17547.

(28) Hong, H.; Jung, Y. H.; Lee, J. S.; Jeong, C.; Kim, J. U.; Lee, S.; Ryu, H.; Kim, H.; Ma, Z.; Kim, T.-i., Anisotropic Thermal Conductive Composite by the Guided Assembly of Boron Nitride Nanosheets for Flexible and Stretchable Electronics. *Adv. Funct. Mater.* **2019**, *29*, 1902575.

(29) Wu, K.; Wang, J.; Liu, D.; Lei, C.; Liu, D.; Lei, W.; Fu, Q., Highly Thermoconductive, Thermostable, and Super-Flexible Film by Engineering 1D Rigid Rod-Like Aramid Nanofiber/2D Boron Nitride Nanosheets. *Adv. Mater.* **2020**, *32*, 1906939.

(30) Maine, E.; Ashby, M. F., Materials Selection and Mechanical Design. In *Encyclopedia of Materials: Science and Technology*, Buschow, K. H. J.; Cahn, R. W.; Flemings, M. C.; Ilschner, B.; Kramer, E. J.; Mahajan, S.; Veyssière, P., Eds. Elsevier: Oxford, 2001; pp 5230-5236.

(31) Maine, E.; Ashby, M. F., Materials Selection and Mechanical Design. In *Reference Module in Materials Science and Materials Engineering*, Elsevier: 2016.

(32) Appendix A - Data for Engineering Materials. In *Materials Selection in Mechanical Design (Fourth Edition)*, Ashby, M. F., Ed. Butterworth-Heinemann: Oxford, 2011; pp 495-523.

(33) Ashby, M. F., Chapter 3 - Engineering Materials and Their Properties. In *Materials Selection in Mechanical Design (Fourth Edition)*, Ashby, M. F., Ed. Butterworth-Heinemann: Oxford, 2011; pp 31-56.

(34) Ashby, M. F., Chapter 15 - Materials and the Environment. In *Materials Selection in Mechanical Design (Fourth Edition)*, Ashby, M. F., Ed. Butterworth-Heinemann: Oxford, 2011; pp 437-459.